Caliphate Journal of Science & Technology (CaJoST)

ISSN: 2705-313X (PRINT); 2705-3121 (ONLINE) Research Article

Open Access Journal available at: https://cajost.com.ng/index.php/files and https://www.ajol.info/index.php/cajost/index

DOI: https://dx.doi.org/10.4314/cajost.v7i3.7

Article Info

Received: 30th July 2025

Revised: 17th September 2025

Accepted: 18th September 2025

Effects of Heat Transfer on Unsteady MHD Blood Flow Through a Tapered and Overlapping Stenosed Artery with Permeable Parameter

Akeem B. Disu[1*], Babatunde A. Joseph[2] and Moses S. Dada[2]

[1]Department of Mathematics, National Open University of Nigeria, Abuja, Nigeria

[2]Department of Mathematics, University of Ilorin, Ilorin, Nigeria

*Corresponding author's email: adisu@noun.edu.ng

Cite this: *CaJoST,* 2025, 3, 361-370

The blood flows through a tapered and overlapping stenosed artery was examined under the influence of magnetic field and porosity. The equations governing the blood flow were formulated and solved analytically. The Nusselt number, resistance to flow, wall shear stress and streamline function were resolved and the results were presented graphically. The result obtained depicted that the viscosity of the blood flow depends on temperature. It was also observed that the velocity of the blood dropped as the magnetic parameter increasing in the velocity profile whereas in the temperature profile, the blood temperature increased under the influence of magnetic parameter. The result showed that the increase of blood temperature could be adversely affected the artery.

Keywords: Heat transfer; permeable, magneto-hydrodynamics, overlapping stenosis, blood flow.

1. Introduction

Blood flow refers to the transportation of blood the vessels from arteries to the capillaries and into the veins. The measurement of the force that the blood exerts against the vessel walls as it carries the blood through the vessels is known as pressure. The enthusiasm for this study is to understand the flowing of porous blood through a stenosed artery. Stenosis occurs when there is abnormal narrowing of blood vessels such as foramina and canals. Narrowing of the blood vessels lead to heart problem ischemic stroke and peripheral intravascular diseases, which is the prime cause of death in the entire world. Babatunde et al., (2021), Azad et al., (2023), Babatude et al., (2025) and Disu et al., (2025) studied the effects of stenosis and aneurysm on blood flow through a post-stenotic artery.

The Bio-magnetic viscoelastic fluid flow and estimation of the blood flow through arteries during electromagnetic hyperthermia studied by Mishra et al., (2010). Therapeutic procedure for cancer treatment was constructed. Malota et al., (2018) used numerical schemes to acquire the impact of heart rate, flow rate, vessel geometry and degree of stenosis on coronary hemodynamic indices.

Hemodynamics is the movement of the blood flow in the body system. The circulatory system is directed by homeostatic mechanisms of auto regulation, just as hydraulic circuits are directed by control systems. The hemodynamic response continuously monitors and adjusts to conditions in the body and its environment. Arteries, Capillaries and Veins are the three main types of blood vessels. The large blood vessels are called arteries which carry blood away from the heart to all other part of the body. The arterioles also split into smaller vessels called capillaries. Capillaries join the arterial and venous circulatory system.

Mathematical examination of blood flow in a permeable vessel is of prodigious concern for physiological investigators and has drawn sincere deliberation of experts. The examination of a porous medium is imperative both from in theoretical and practical point of view. Mekheimer and AlArabi (2003) studied the mathematical model to decide the attributes of peristaltic move of MHD flow through a permeable medium. Misra and Verma (2007) investigated the numerical method for the impact of permeable parameter and stature stenosis on the divider shear stress

Many researchers examined movement of MHD blood flow through stenosed arteries. Bansal (1976) found an important role of external magnetic field plays on various biological systems of the body. The applied magnetic field provides an effective kind of medical treatment on the human bodies. Early Japan, hypertension and neurasthenia patients are treated by application of magnetic belt, cap, pillow and bed. It is found that magnetic treatment cures the hypertension, coronary thrombosis, angina pectoris and high blood-lipoid.

Victor and Shah (1976) studied the steady state heat transfer of the blood flow in the entrance region of a tube. Zhonggang and Wangyi (1995) investigated the thrombus and other blood rheological properties with an applied magnetic field. The effects of magnetic field on the pulsatile flow through a rigid tube were measured. They observed that the constant magnetic field barricades the blood circulation and that the magnetic field is less active for the large vessels. Mazumdar et al (1996) constructed magnetic effects on Newtonian fluid in a circular tube with numerical method. They found that the fluid viscosity is always constant and vary in term of temperature and pressure. Tzirtzilakis and Loukopoulos (2005) demonstrated mathematical model for blood flow with magnetic field parameter. The blood flow in small vessel with the aid of magnetic field was studied by Gupta (2012). Ahmad and Ahmad (2012) investigated the effect of blood flow through renal tube. They got the results of periodic blood fluid distribution and profile velocity component. Sharma and Katiyar (2015) investigated the magnetic effects on blood flow in cylindrical tube. Bunonyo et al., (2018) studied the oscillatory blood flow in a stenosed artery with heat source in the presence of magnetic field. Tripathi and Sharma (2018) examined the effect of chemical reaction and variable viscosity on MHD inclined arterial blood flow. Ahmad et al., (2021) constructed the effect of magnetic and perturbation parameters on blood flow distribution through an artery. They observed that the temperature and shear stress of the blood rises with respect to perturbation and magnetic field. Hanvey and Bunonyo (2022) effect of treatment parameter on oscillatory flow of blood through an atherosclerotic artery with heat transfer.

The sewing of a layer of tissue above or under another in order to gain strength is called overlapping. Chakravarty and Mandal (1994) examined the Mathematical modelling of blood flow through an overlapping stenosed artery. Found that the rigorousness of the overlapping stenosis affects the wall shear stress. Babatunde and Dada (2021) investigated the effect of hematocrit level on blood flow through a tapered and overlapping stenosed with permeable wall. Babatunde and Dada (2023) studied the magnetic effects on unsteady Non-Newtonian blood flow through a tapered and overlapping stenotic artery.

The study considers an unsteady viscous incompressible laminar and Newtonian fluid problem through a horizontal tube with radius; the cylindrical coordinate system is introduced in **Fig.** 1. Let the three components of velocities along the radius, perpendicular to the radius vector, and parallel to the axis of x, be w^r,w^θ, and w^x respectively.

2. Mathematical model

The study considers a laminar, incompressible and Newtonian fluid problem through axisymmetric unidirectional model of tapered and overlapping stenosed artery under the effect of external magnetic field. We further considered variable viscosity depends on temperature. Here the Reynold's number regime is very low $(Re \ll 1)$. When the operating Reynolds number is low, inertial force is negligible as compared to viscous force which is called creeping flows. Any material point in the fluid is represented by the cylindrical polar coordinate (r, θ, z), where z is coordinate along the axis of the artery, while r and θ are coordinates along the radial and circumferential directions, respectively.

The mathematical expression for unsteady flow that corresponds to the geometry in Fig. 1 is given by Mekheimer and Kot (2015).

$$R(z,t) = \Big\{(mz + R_0)\vartheta(t) - \frac{\delta cos\emptyset}{L_0}(z-d)\Big\{11 - \frac{94}{3L_0}(z-d) + \frac{32}{L_0^2}(z-d)^2 - \frac{32}{3L_0^3}(z-d)^3\Big\}\vartheta(t), d \le z \le d + \frac{3L_0}{2} (mz + R_0)\vartheta(t), \quad \text{otherwise} \qquad (1)$$

$$\vartheta(t) = 1 - a(\cos\omega t - 1)e^{-a\omega t} \qquad (2)$$

where $R(z,t)$ represents the radius of the tapered artery in the restricted region, R_0 denotes the constant radius of the artery in the non-stenotic region, φ is the angle of tapering, $\frac{3L_0}{2}$ the length of overlapping stenosis, $\delta cos\varphi$ represents the critical height of the overlapping stenosis, d is the location of the stenosis and $m = tan\varphi$ is the angle of the tapered artery. To see the in sightsee of the different kind of shapes associated with the vessel, $(\varphi < 0)$ taken as convergence tapering, $(\varphi = 0)$ non-tapered and $(\varphi > 0)$ the divergence tapering. $\vartheta(t)$ denotes the time variant parameter, a is a constant, ω represents the angular frequency of the forced oscillation and t is the time.

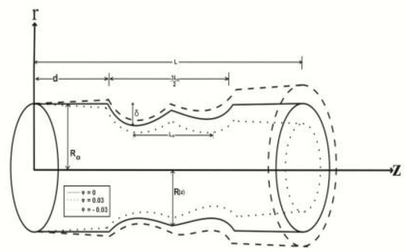

Fig.1. Schematic diagram of overlapping stenosed artery.

3. Mathematical Formulation

The momentum and energy equations for a fully developed flow of blood through a cylindrical tube, when the wall of the tube is kept at a constant temperature, we have:

$$\rho\frac{\partial \bar{w}^z}{\partial \bar{t}} = -\frac{\partial \bar{p}}{\partial \bar{z}} + \mu\left(\frac{\partial^2 \bar{w}^z}{\partial \bar{r}^2} + \frac{1}{\bar{r}}\frac{\partial \bar{w}^z}{\partial \bar{r}}\right) - \frac{\mu \bar{w}^z}{k'} + \beta_0^2\sigma\bar{w}^z \quad (3)$$

$$\frac{\partial \bar{T}}{\partial \bar{t}} = \frac{k_T}{\bar{r}}\left(\frac{\partial^2 \bar{T}}{\partial \bar{r}^2} + \frac{1}{\bar{r}}\frac{\partial \bar{T}}{\partial \bar{r}}\right) + \mu\left(\frac{\partial \bar{w}^z}{\partial \bar{r}}\right)^2 \quad (4)$$

The corresponding boundary conditions are given as:

$\bar{w}^z = 0, \bar{T} = \bar{T}_w$ at $\bar{r} = \bar{R}(z,t)$, (no-slip condition) (5)

$\bar{w}^x = 0,\ \bar{T} = \bar{T}_w$ at $\bar{r} = 0, \bar{t} \geq 0,$

The following dimensionless parameters are used to simplify the governing equations as follows:

$$z = \frac{\bar{z}}{\lambda}, \eta = \frac{\bar{r}}{R_0}, w = \frac{\bar{w}^z}{w_m}, Da = \frac{k'}{R_0^2}, M = \beta_0 R_0\sqrt{\frac{\sigma}{\mu_0}},$$
$$t = \frac{\bar{t}w_m}{R_0}, Re = \frac{\rho w_m R_0}{\mu}, p = \frac{\bar{p}R_0^2}{\rho\upsilon\lambda w_m},\ \mu = \rho\upsilon, \quad (6)$$
$$T = \frac{\bar{T}-\bar{T}_0}{\bar{T}_w-\bar{T}_0} = \frac{\bar{T}_w-\bar{T}}{\bar{T}_0}, E_c = \frac{w_m^2}{C_p(T_w-\bar{T}_0)}, Pr = \frac{\mu_0 C_p}{k}, \bar{m} = \frac{m\lambda}{R_0} = \tan\varphi,$$
$$h = \frac{R(z,t)}{R_0}, \bar{\delta} = \frac{\delta\cos\emptyset}{\lambda R_0}$$

where Pr is the Prandtl number of the fluid, E_c is dimensionless quantity, Br is Brickmann number, k denotes the thermal conductivity, ρ is the density, p is the blood pressure, Re represents Reynolds number, $\bar{T}$ is the local temperature of the flow, μ is the blood viscosity, C_p is the specific heat, Da is Darcy number and $\bar{T}_0$ is the temperature of the blood at the stenotic region, $\bar{z}$ is the dimensional axial position (mm), η is the dimensional radial position (mm), w is the velocity (m/s), w_m is the average velocity (m/s), t is the time, ω is the oscillating frequency (rad/s). The Non-dimensional variables are represented without bar.

Substituting Equation (6) into Equations (1) to (5), resulted to the non-dimensional form as:

$$\mathrm{Re}\left(\frac{dw}{dt}\right) = -\frac{\partial p}{\partial z} + \left(\frac{\partial^2 w}{\partial \eta^2} + \frac{1}{\eta}\frac{\partial w}{\partial \eta}\right) - \left(\frac{1}{Da} + M^2\right)w \quad (7)$$

$$Pr\frac{\partial T}{\partial t} = \left(\frac{\partial^2 T}{\partial \eta^2} + \frac{1}{\eta}\frac{\partial T}{\partial \eta}\right) + PrE_c\left(\frac{\partial w}{\partial \eta}\right)^2, \quad (8)$$

$$h(z,t) = \left\{\left[(\bar{m}z+1) - \bar{\delta}(z-d)\left\{11 - \frac{94}{3L_0}(z-d) + \frac{32}{L_0^2}(z-d)^2 - \frac{32}{3L_0^3}(z-d)^3\right\}\right]\vartheta(t), d \leq z \leq d + \frac{3L_0}{2}\ (\bar{m}z+1)\vartheta(t),\ \text{otherwise}\right. \quad (9)$$

where $\vartheta(t) = 1 - a(\cos\omega t - 1)e^{-a\omega t}$

with the boundary conditions

$w = 0,\ T = 1$ at $\eta = h(z,t)$, (no-slip condition) (10)

$w = 0, T = 0$ at $\eta = 0, t \geq 0$ (11)

4. Mathematical Analysis

Pulsatile pressure gradient may be expressed in terms of frequency and time limit for an unsteady state.

$$\frac{\partial p}{\partial z} = -P_0 e^{i\omega t}, \quad (12)$$

the pumping action of the heart gives rise to oscillatory flow of the blood, we assume

$$w(r,t) = w(r)_0 e^{i\omega t} \quad (13)$$

$$T(r,t) = T(r)_0 e^{i\omega t} \quad (14)$$

where P_0 is the pressure constant and ω is the angular oscillating frequency.

$$\left(\frac{\partial^2 w_0}{\partial \eta^2} + \frac{1}{\eta}\frac{\partial w_0}{\partial \eta}\right) - \varpi^2 w_0 = -P_0 \quad (15)$$

$$\left(\frac{\partial^2 T_0}{\partial \eta^2} + \frac{1}{\eta}\frac{\partial T_0}{\partial \eta}\right) - Br\left(\frac{\partial w_0}{\partial \eta}\right)^2 = Pri\omega t \quad (16)$$

The corresponding boundary conditions:

$w_0 = 0,\ T_0 = e^{-i\omega t}$ at $\eta = h(z,t)$, (no-slip condition)

$w_0 = 0, T_0 = 0$ at $\eta = 0, t \geq 0,$ (17)

where, $\varpi^2 = \left(M^2 + \frac{1}{Da} + Rei\omega\right)$

Now, the homogeneous solution of Equation (15) is:

$$\left(\frac{\partial^2 w_0}{\partial \eta^2} + \frac{1}{\eta}\frac{\partial w_0}{\partial \eta}\right) - \varpi^2 w_0 = 0 \quad (18)$$

The above Equation (18) is a modified Bessel differential equation; therefore its solution can be given as:

$$w_{0h}(\eta) = AI_0(\varpi\eta) + BK_0(\varpi\eta) \quad (19)$$

Here, $B = 0$, as the solution is bounded at $\eta = 0$, therefore Equation (19) will reduce to:

$$w_{0h}(\eta) = AI_0(\varpi\eta) \quad (20)$$

Now, solving Equation (15) to the particular solution by using the method of undetermined coefficients, we have:

$$w_{0p}(\eta) = \frac{P_0}{\varpi^2} \quad (21)$$

The general solution is obtained by adding Equations (20) and (21) together:

$$w_{0g} = AI_0(\varpi\eta) + \frac{P_0}{\varpi^2} \quad (22)$$

In order to solve arbitrary coefficient A in Equation (22), the boundary condition based on Equation (17) can be modified as:

$$A = -\frac{P_0}{\varpi^2} \quad (23)$$

The complete solution of Equation (23) in terms of non-dimensional pulsating velocity profile as a function of non-dimensional radial position can be obtained as:

$$w_{0g} = -\frac{P_0}{\varpi^2} I_0(\varpi\eta) + \frac{P_0}{\varpi^2} \quad (24)$$

Hence, unsteady state the velocity profile is given as:

$$w_{0g}(\eta, t) = \frac{P_0}{\varpi^2} e^{i\omega t}\left(1 - I_0(\varpi\eta)\right) \quad (25)$$

Substitute Equation (24) into Equation (16), we have:

$$\frac{1}{\eta}\frac{\partial}{\partial\eta}\left(\eta\frac{\partial T_0}{\partial\eta}\right) = Pri\omega t + Br\left(\frac{P_0}{\varpi^2} - \frac{P_0}{\varpi^2} I_0(\varpi\eta)\right)^2 \quad (26)$$

Integrating Equation (26) with respect to η, we have

$$\frac{\partial T_0}{\partial\eta} = \frac{Pri\omega t\eta}{2} + \frac{BrP_0^2 e^{i\omega t}\eta}{2\varpi^4} + \frac{2BrP_0^2 e^{i\omega t}\eta I_1(\varpi\eta)}{\varpi^3} + \frac{\left[\left(I_0(\varpi\eta)\right)^2 - \left(I_1(\varpi\eta)\right)^2\right]BrP_0^2 e^{i\omega t}\eta}{2} + \frac{C}{\eta} \quad (27)$$

Applying the boundary conditions on equation (17) and with $C \neq 0$, the expression in RHS will be undefined. Therefore, $C = 0$ and

$$\frac{\partial T_0}{\partial\eta} = \frac{Pri\omega t\eta}{2} + \frac{BrP_0^2 e^{i\omega t}\eta}{2\varpi^4} + \frac{2BrP_0^2 e^{i\omega t}\eta I_1(\varpi\eta)}{\varpi^3} + \frac{\left[\left(I_0(\varpi\eta)\right)^2 - \left(I_1(\varpi\eta)\right)^2\right]BrP_0^2 e^{i\omega t}\eta}{2} \quad (28)$$

Integrating equation (28) and applying the boundary condition (17) to get

$$T_0 = \frac{Pri\omega t e^{i\omega t}(\eta^2 - h^2)}{2} + \frac{BrP_0^2 e^{2i\omega t}(\eta^2 - h^2)}{4\varpi^4} + \frac{2BrP_0^2 e^{2i\omega t}\left(I_0(\varpi\eta) - I_0(\varpi h)\right)}{\varpi^3} + \frac{\left[\eta^2\left(I_0(\varpi\eta)\right)^2 - h^2\left(I_0(\varpi\eta)\right)^2\right]BrP_0^2 e^{2i\omega t}}{4} - \frac{\left[\eta^2\left(I_1(\varpi\eta)\right)^2 - h^2\left(I_1(\varpi\eta)\right)^2\right]BrP_0^2 e^{2i\omega t}}{2} + \frac{\left[\eta^2\left(I_0(\varpi\eta)\right) - h^2\left(I_0(\varpi\eta)\right)\right]\left(\left(I_2(\varpi\eta)\right) - \left(I_2(\varpi\eta)\right)\right)BrP_0^2 e^{2i\omega t}}{4} \quad (29)$$

The streamline function is given as:

$$\psi = \int_0^{h(z,t)} \eta w_0(\eta, t)\, d\eta \quad (30)$$

Substituting Equation (25) into Equation (30)

and integrate, we get:

$$\psi = \frac{P_0 e^{i\omega t} h^2(z,t)}{2\varpi^2} - \frac{P_0 e^{i\omega t} h(z,t) I_1(\varpi h(z,t))}{\varpi^3} \quad (31)$$

Nusselt number (Nu) is defined as:

$$Nu = \left.\frac{\partial T}{\partial\eta}\right|_{\eta = h(z,t)} \quad (32)$$

Substituting Equation (28) into Equation (32), we get:

$$Nu = \frac{Pri\omega t h(z,t)}{2} + \frac{BrP_0^2 e^{i\omega t} h(z,t)}{2\varpi^4} + \frac{2BrP_0^2 e^{i\omega t}\eta I_1(\varpi h(z,t))}{\varpi^3} + \frac{\left[\left(I_0(\varpi h(z,t))\right)^2 - \left(I_1(\varpi h(z,t))\right)^2\right]BrP_0^2 e^{i\omega t} h(z,t)}{2} \quad (33)$$

The flux flow rate is given as

$$Q = 2\pi\int_0^{h(z,t)} \eta w(\eta, t)\, d\eta \quad (34)$$

After simplifying Equation (34), it becomes

$$Q = -\frac{\pi h(z,t)}{\varpi^2}\frac{dp}{dz}\left[h(z,t) - \frac{2I_1(\varpi h(z,t))}{\varpi}\right] \quad (35)$$

Therefore, the pressure gradient from Equation (35) is

$$\frac{dp}{dz} = \frac{\varpi^3 Q}{\pi h(z,t)\left(\varpi h(z,t) - 2I_1(\varpi h(z,t))\right)} \quad (36)$$

Integrating Equation (36) along the length of the artery, we have

$$\int_{p_0}^{p_1}\frac{dp}{dz} = \int_0^L \frac{\varpi^3 Q}{\pi h(z,t)\left(\varpi h(z,t) - 2I_1(\varpi h(z,t))\right)}\, dz \quad (37)$$

The pressure drop

$$\Delta p = \frac{Q\varpi^3}{\pi}\int_0^L \frac{1}{h(z,t)\left(\varpi h(z,t) - 2I_1(\varpi h(z,t))\right)}\, dz \quad (38)$$

where $p_0$and $p_1$are the pressures at z=0 and z=L respectively.

$$p_1 - p_0 = \frac{\varpi^3 Q}{\pi}\left\{\int_0^d V(z)\, dz + \int_d^{d+\frac{3L_0}{2}} V(z)\, dz + \int_{d+\frac{3L_0}{2}}^L V(z)\, dz\right\} \quad (39)$$

where $V(z) = \frac{1}{h(z,t)\left(\varpi h(z,t) - 2I_1(\varpi h(z,t))\right)}$

The resistance to flow λ given by (Babatunde and Dada, 2021) as

$$\lambda = \frac{p_1 - p_0}{Q}$$

Hence,

$$\lambda = \frac{\varpi^3}{\pi}\left\{\int_0^d V(z)\, dz + \int_d^{d+\frac{3L_0}{2}} V(z)\, dz + \int_{d+\frac{3L_0}{2}}^L V(z)\, dz\right\} \quad (40)$$

The stenosis is present in the region $d \leq z \leq d + \frac{3L_0}{2}$. If there is no stenosis $h(z,t) = (\frac{mz}{R_0} + 1)\theta(t)$ from Equations (1). Therefore,

$$\lambda = \frac{\varpi^3}{\pi}\left\{\int_0^d \zeta(z)\, dz + \int_d^{d+\frac{3L_0}{2}} V(z)\, dz + \int_{d+\frac{3L_0}{2}}^L \zeta(z)\, dz\right\} \quad (41)$$

where,

$$\zeta(z) = 1/\left(\left(\frac{mz}{R_0}+1\right)(1-a(\cos\omega t-1)e^{-a\omega t})\left[\varpi\left(\frac{mz}{R_0}+1\right)(1-a(\cos\omega t-1)e^{-a\omega t})-2I_1\left(\varpi\left(\frac{mz}{R_0}+1\right)(1-a(\cos\omega t-1)e^{-a\omega t})\right)\right]\right)$$

The resistance to flow when there is no stenosis ($\delta=0$) is given by

$$\lambda_N = \frac{\varpi^3}{\pi}\int_0^L \zeta(z)dz \quad (42)$$

Thus, the dimensionless resistance to flow may be expressed as

$$\bar{\lambda} = \frac{\lambda}{\lambda_N} \quad (43)$$

The wall shear stress may be expressed as

$$\tau_s = -\frac{h(z,t)}{2}\frac{dp}{dz} = \frac{\varpi^3 Q}{2\pi(\varpi h(z,t)-2I_1(\varpi h(z,t)))} \quad (44)$$

The wall shear stress when there is no stenosis ($\delta=0$) is given as

$$\tau_N = \varpi^3 Q/\left(2\pi\left[\varpi\left(\left(\frac{mz}{R_0}+1\right)(1-a(\cos\omega t-1)e^{-a\omega t})\right)-2I_1\left(\varpi\left(\left(\frac{mz}{R_0}+1\right)(1-a(\cos\omega t-1)e^{-a\omega t})\right)\right)\right]\right) \quad (45)$$

Thus, the wall shear stress in non-dimension form is expressed as

$$\bar{\tau} = \frac{\tau_s}{\tau_N}$$

5. Results and Discussion

In order to shown the solution for this work, the graphical results are presented. In this section, effects of heat transfer on unsteady magnethohydrodynamic blood flow through a tapered and overlapping stenosed artery with porosity had been explode. The values of human blood taken as $37°C$. Chato (1980), Chaturani and Bharatiya (2001), Ahmad et al. (2021) and Babatunde and Dada, (2023), the physiological data has been considered as follows:
$\mu = 3.2\times10^{-3}m^{-1}s^{-1}, \sigma = 1.4mho.m^{-1},\ \mu_0 = 1.2\times10^{-3}m^{-1}s^{-1}, \rho = 1050kgm^{-3}, k = 2.2\times10^{-3}jm^{-1}s^{-1}K, C_p = 14.65jKg^{-1}K^{-1}, R = 0.4\times10^{-2}m, w_m = 90\times10^{-2}ms^{-1}, \beta = 0.021°C^{-1}, T_0 = 310K, B_0 = 8T(Tesla), Q = 0.1s^{-1}$, L = 2.5mm, $L_0 = 1.0mm$, d = 0.5mm, $R_0 = 0.5mm$.
From the physiological values above, we get the approximate values of Prandtl number, $Pr = \frac{\mu_0 C_p}{k} \cong 8.79 \approx 9$, Eckert number, $E_c = \frac{w_m^2}{C_p\bar{T}_0} \cong 1.79\times10^{-4}$, magnetic parameter, $M = \beta_0 R_0\sqrt{\frac{\sigma}{\mu_0}} \cong 1.1$, and

Brickman number, $Br = PrE_c \cong 1.57341\times10^{-3} \approx 0.00157 \ll 1$.

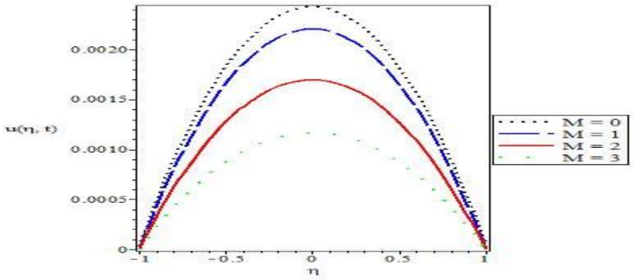

Fig. 2. Velocity profile variation for the magnetic field.

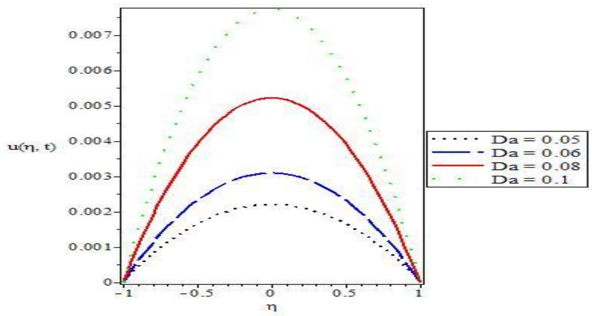

Fig. 3. Velocity profile variation for the Darcy number.

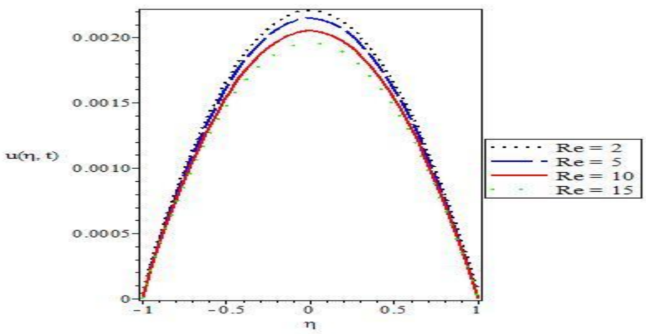

Fig. 4. Velocity profile variation for the Reynolds number.

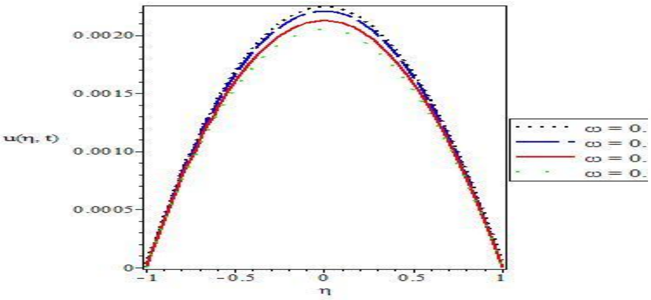

Fig. 5. Variation of velocity for different oscillating frequency.

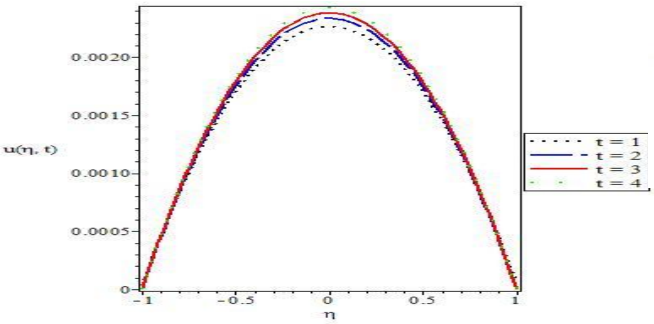

Fig. 6. Velocity against radial direction for different time taken.

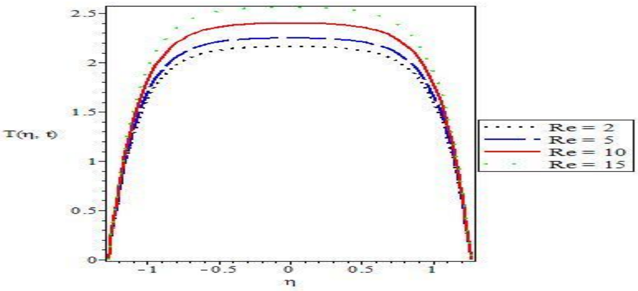

Fig. 7. Temperature against radial direction for different Reynolds number for $\varphi = 0.03$.

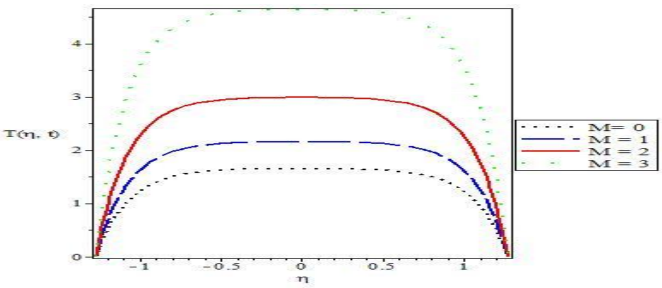

Fig. 8. Temperature against radial direction for different magnetic field for $\varphi = 0.03$.

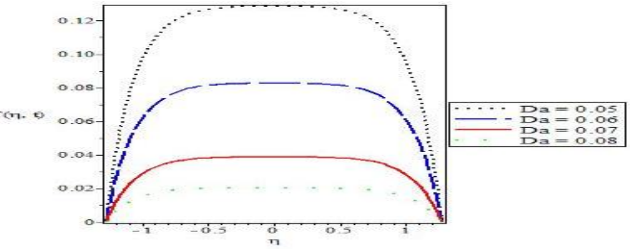

Fig. 9. Temperature against radial direction for different Darcy number $\varphi = 0.03$.

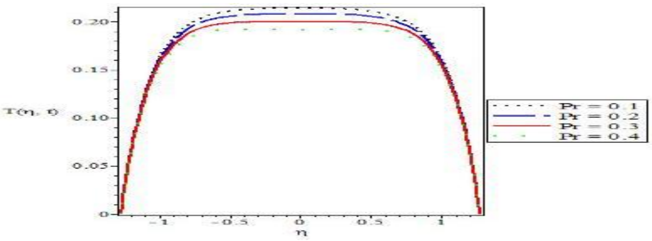

Fig. 10. Temperature against radial direction for different Prandlt number

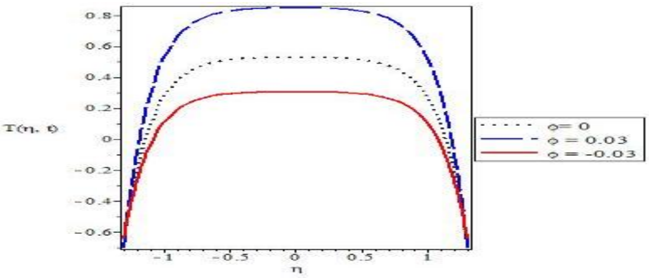

Fig. 11. Temperature against radial direction for different tapered angles

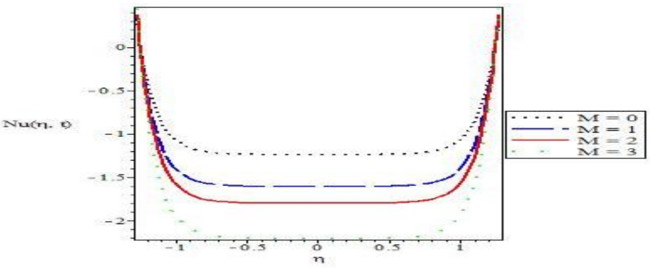

Fig. 12. Nusselt number against radial direction for different magnetic field

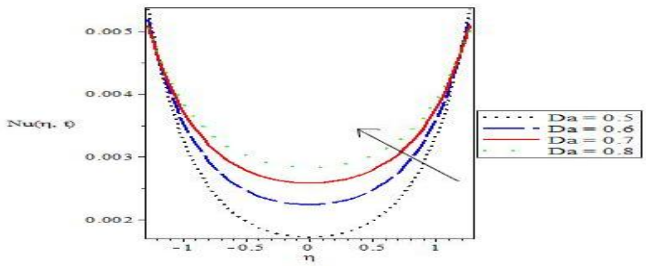

Fig. 13. Nusselt number against radial direction for different Darcy number

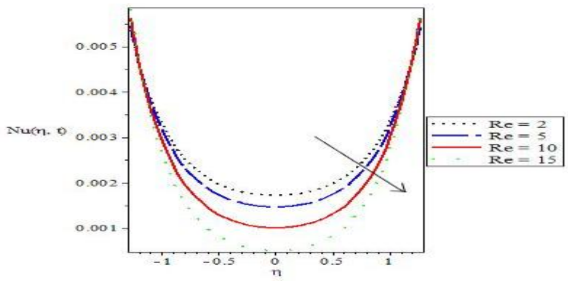

Fig. 14. Nusselt number against radial direction for different Reynolds number

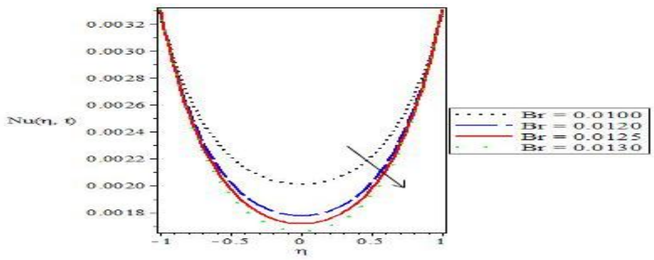

Fig. 15. Nusselt number against radial direction for different Brickman number

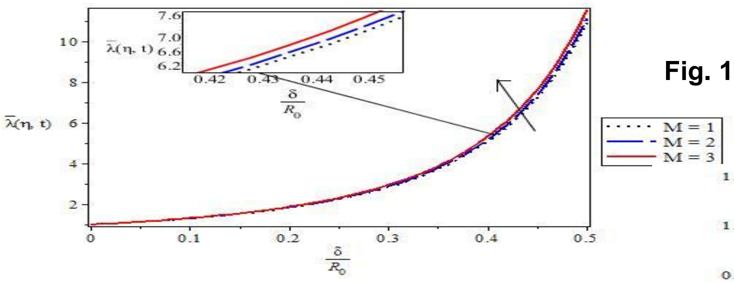

Fig. 16. Dimensionless resistance against stenosis height for different magnetic field

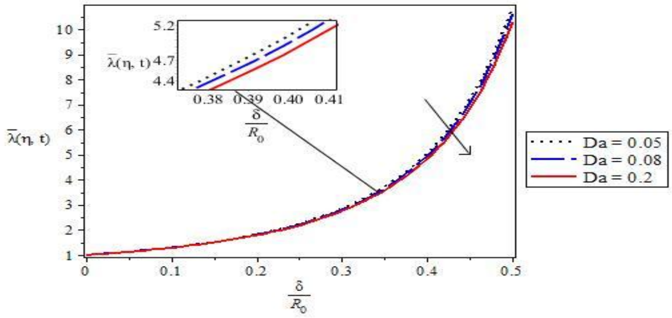

Fig. 17. Dimensionless resistance against stenosis height for different Darcy number

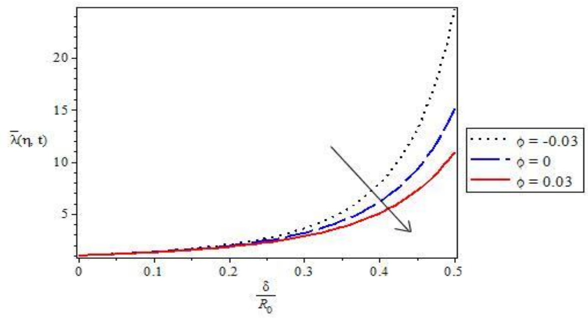

Fig. 18. Dimensionless resistance against stenosis height for different tapered angles

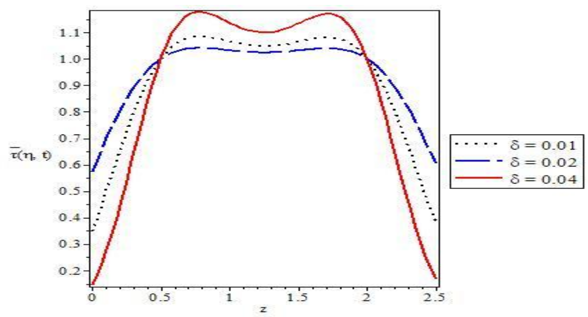

Fig. 19. Dimensionless wall shear stress against z for different stenosis height

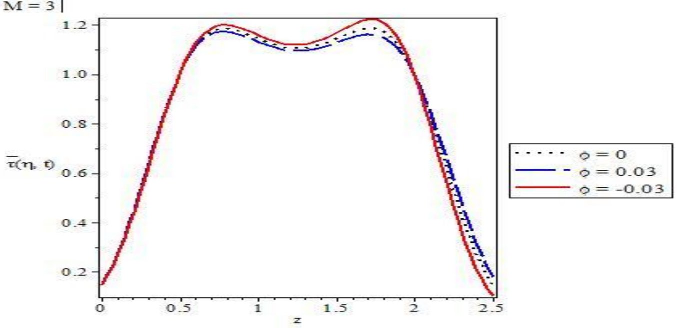

Fig. 20. Dimensionless wall shear stress against z for different tapered angles

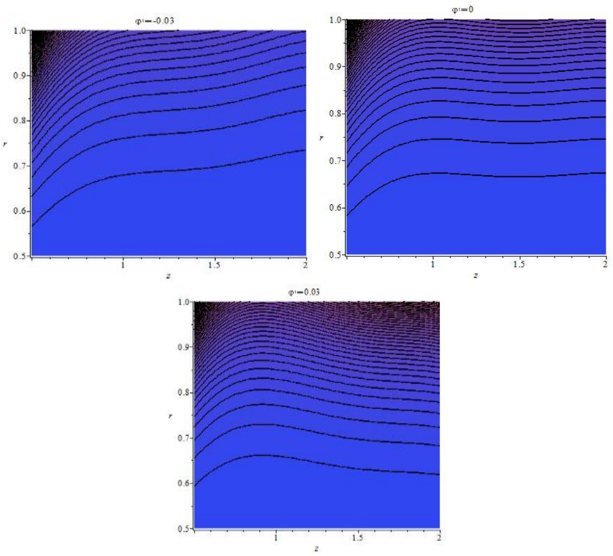

Fig. 21. Stream line for different tapered angles

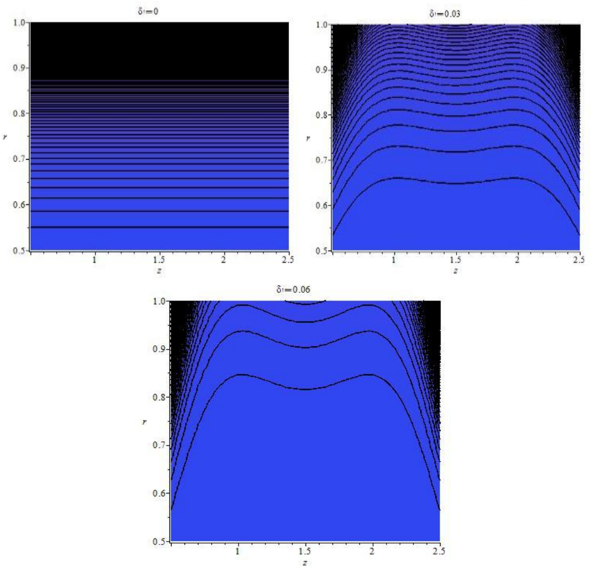

Fig. 22. Stream line for different stenosis height

Figs. (2-5) display the graphs of velocity profile against radial direction for different fluid parameters such as magnetic field, Darcy number, Reynolds number, oscillating frequency and time taken for diverging taper angle $(\varphi = 0.03)$. It is observed that velocity profile rises by increasing the radial direction, Darcy number and time while it decreases by increasing the magnetic field, oscillating frequency and Reynolds number.

Figs. (6-11) show the graphs of temperature profile against radial direction for different fluid parameters such as Reynolds number, magnetic field, Darcy number, Prandlt number and tapered angle. It is observed that temperature profile upsurges as the radial direction, Reynolds number, magnetic field and tapered angle rise but it reduces by increasing the Darcy number and Prandlt number.

Figs. (12-15) illustrate the graphs of Nusselt number against radial direction for magnetic field, Darcy number, Reynolds number and Brickman number. It is found that Nusselt number upsurges as the Brickman number, magnetic field and Reynolds number decrease but it rises by increasing the Darcy number.

Figs. (16-18) represent the graphs of resistance to flow against stenosis height for magnetic field, Darcy number and taper angle. It is observed that resistance to flow increases as the stenosis height, magnetic field and tapered angle rise but it reduces by increasing the Darcy number.

Fig. 19 displays the graph of wall shear stress against z-direction for different value of stenosis height. It is found that wall shear stress increases with rising in z-direction, it decreases by increasing the stenosis height in non-stenotic region but converse is the case at a stenotic region. Fig. 20 shows the graph of wall shear stress against z-direction for different value of tapered angle. It is found that wall shear stress increases with rising in z-direction, it increases by increasing the tapered angle in non-stenotic region but converse is the case at a stenotic region.

Figs. 21 represents the streamline of the blood flow in the artery for tapered angle. There is a shifting up of the fluid flow near the artery wall for convergence $(\varphi = -0.03)$, the fluid flows normal for non-tapered $(\varphi = 0)$and shifts downwardly near the artery wall for divergence $(\varphi = 0.03)$. Fig. 22 illustrates the streamline of the blood flow in the artery for stenosis height. It is observed that there is a straight flow when there is no stenosis and increases in trapped bolus as the stenosis height increasing.

6. Conclusion

The effect of heat transfer on unsteady magnetodynamic blood flow through a tapered and overlapping stenosed artery with porosity is studied. This study permits one to understand the roles of red blood cells on flow characteristics in a tapered overlapping stenosis. The graphical illustrations are shown for the velocity profile, temperature profile, Nusselt number, resistance to flow, wall shear stress and streamline function. The results are summarized as follows:

1. It is found that velocity profile accelerates by increasing the Darcy number and oscillating frequency.
2. The velocity of the blood drops as the magnetic parameter hakes but the temperature profile of the blood increases under the influence of magnetic field. It occurs

as the effect of magnetic field on blood flow accelerates the internal viscosity of the blood flow which causes increase to the Lorentz force. This situation is hazardous, because the increase of blood temperature will destroy oxygenation of blood in hemodialysis.

3. It is observed that Nusselt number increases as the Brickman number, magnetic field and Reynolds number move downward.
4. The flow resistance increases as the stenosis height, magnetic field and tapered angle increase.
5. The wall shear stress increases by increasing the stenosis height in stenotic region but convers is the case for non-stenotic region.

References

Ahmad, S. and Ahmad, N. (2012). On flow through renal tubule in case of periodic radial velocity component, Int. Journal of Emerging Multidisciplinary Fluid science, 3(4), 201-108. https://doi.org/10.1260/1756-8315.3.4.201

Ahmad, Sultan, Al-Johani, A.F. and Sahu, Subrata Kumar, (2021) Effect of magnetic and perturbation parameters on blood flow distribution through an artery. Applications and Applied Mathematics: An International Journal (AAM), Vol. 16, Issue 1, (32), ISSN: 1932-9466.

Azad, H., Muhammad Naveel R. Dar and Elsayed M. T., (2023) Effects of stenosis and aneurysm on blood flow in stenotic-aneurysmal artery. Heliyon, (9) e17788.https://doi.org/10.1016/j.heliyon.2023.e1778

Babatunde A. J., Dada M. S., Bello A. J. F., Disu, A. B., Alamu-Awoniran, F. H. and Dana J. Y. (2025). Effect of stenotic-aneurysmal arterial regime on unsteady magnetohydrodynamic non-Newtonian blood flow with heat radiation. Applications and Applied Mathematics: An International Journal (AAM), Vol 20, Issue 1(20) ISSN: 1932-9466.

Babatunde A. J. and Dada M. S. (2023), Magnetic Effects on Unsteady Non-Newtonian Blood Flow through a Tapered and Overlapping Stenotic Artery, Applications and Applied Mathematics: An International Journal (AAM), Vol. 19, Issue 1, (6), ISSN: 1932-9466.

Babatunde A. J. and Dada M. S., 2021. Effects of Hematocrit level on Blood flow through a tapered and overlapping stenosed Artery with Porosity. JHMTR, (1-9), 2007-1293.

Babatunde, A. J., Oyekunle T. L., Danas J. Y. and Mohammed M. T., (2021). Effects of hematocrit and heat transfer in magnetohydrodynamic blood flow through a vertically tapered and overlapping stenosed artery, JOSIT

Bunonyo, K.W., Isreal-Cookey C. and Amos E. Modeling of blood flow through stenosed artery with heat in the presence of magnetic field, Asian Research Journal of Mathematics, 8(1): 1-14, ISSC: 2456-477X. https://doi.org/10.9734/ARJOM/2018/37767

Bansal M.L. (1976). Magneto therapy, Jain Publishers, New Delhi.

Chakravarty. S. and Mandal P. K., (1994). Mathematical modelling of blood flow through an overlapping Arterial stenosis. Math. & Comp. Modelling, Vol.19, Issue 1, page 59-70. https://doi.org/10.1016/0895-7177(94)90116-3

Chato, J.C. (1980). Heat Transfer to Blood Vessels, Journal of Biomedical Engineering, 102, 110-118.

Chaturani, P. and Saxena Bharatiya, S. (2001). Two layered magneto-hydrodynamic flow through parallel plates with applications, Indian Journal Pure and Applied Mathematics, 32 (1), 55-68.

Disu A. B.,Babatunde A. J., Alamu-Awoniran F. H., Bello A. J. F. Mohammed M. T. and Danas J. Y. (2025). Hemorhelogy of blood flow infused with alumina and ferric oxide nanoparticles through an inclined permeable tapered and overlying stenosed artery. International Journal of Engineering Research and Development,Vol 21,(6), 11-24.

Feng Zhonggang and Wu Wangyi (1995). Effect of the magnetic field on the pulsatile flow through a rigid tube, Applied Mathematics and Mechanics, Vol. 16, pg. 521-532.

Gupta, A.K. (2012). Performance model and analysis of blood in small vessel with magnetic effects. IJET Transactions A, 25 (2), 189-196.

Hanvey R.R. and Bunonyo K. W., (2022) Effect of treatment parameter on oscillatory flow of blood through an atherosclerotic artery with heat transfer, Journal of the Nigerian Society of Physical Sciences, (4) 682. https://doi.org/10.46481/jnsps.2022.682

Mazumdar, H.P., Ganguly, U.N., Venkatesan, S.K. (1996). Some effects of a magnetic field on the flow of a Newtonian fluid through a circular tube, Indian Journal Pure and Applied Mathematics, **27** (5), 519-524.

Malota et al. (2018). Numerical analysis of the impact of flow rate, heart rate, vessel geometry and degree of stenosis on coronary hemodynamic indices, BMC Cardiovascular Disorders, 18, 132.

Mekheimer KS, Al-Arabi TH (2003). Nonlinear peristaltic transport of MHD flow through a porous medium. International Journal of Mathematics and Mathematical Sciences. (26):1663-82. **http://eudml.org/doc/44738**

Mekheimer Kh. S. and El Kot M.A. (2015). Suspension model for blood flow through catheterized curved artery with time-variant overlapping stenosis, Engineering Science and Technology, an International Journal, 1-11.

Misra M, Mittal M, Singh RK, Verma AM, Rai R, Chandra G, Singh DP, Chauhan R, Chowdhary

V, Mall A, Khan MJ. (2007) Prevalence of rheumatic heart disease in school-going children of Eastern Uttar Pradesh. Indian Heart Journal. 59(1):42-3**.**

Mishra, J.C. Sinha, A. and Shit, G.C. (2010). Flow of a bio-magnetic viscoelastic fluid: application to estimation of blood flow in arteries during electromagnetic hyperthermia, a therapeutic procedure for cancer treatment, Applied